ELSEVIER

Journal of Organometallic Chemistry 488 (1995) 141–154

Journal of Organometallic Chemistry

A novel class of hexanuclear titanoxanes: synthesis, structure and electronic configuration [☆]

Tommaso Carofiglio [a], Carlo Floriani [a,*], Alan Roth [b], Antonio Sgamellotti [c], Marzio Rosi [c], Angiola Chiesi-Villa [d], Corrado Rizzoli [d]

[a] *Institut de Chimie Minérale et Analytique, Université de Lausanne, Place du Château 3, CH-1005 Lausanne, Switzerland*
[b] *Department of Chemistry, Columbia University, New York, NY 10027, USA*
[c] *Dipartimento di Chimica, Università di Perugia, Via Elce di Sotto 8, I-06100 Perugia, Italy*
[d] *Dipartimento di Chimica, Università di Parma, Viale della Scienze, I-43100 Parma, Italy*

Received 16 June 1994

Abstract

Reduction of cyclopentadienyloxochloro complexes such as $[\text{R-cpTiCl}(\mu_2\text{-O})]_4$ (R = H (**1**), Me (**2**) or $SiMe_3$ (**3**)) with a variety of reducing agents (Zn, Na, Mg or LiN_3) in tetrahydroforum gave the hexanuclear titanoxanes $[(\text{R-cp})_6Ti_6O_6Cl_2]$ (R = H (**4**), Me (**5**) or $SiMe_3$ (**6**)) with a good yield. Complexes **4–6** are soluble in organic solvents, are diamagnetic and contain four electrons more than are required for the existence of the hexanuclear skeleton. Complex **4** was equally satisfactorily obtained by reducing $[\text{R-cpTiCl}_2(\mu_2\text{-O})]$ (R = H) (**7**) will Bu_3SnH. Reduction of **1** and **2** with Al powder gave $[\text{R-cp}_6Ti_6O_4Cl_4]$ (R = H (**8**) or Me (**9**)). They contain two unpaired electrons. Reaction of H_2O with **4** and **5** gave the diamagnetic titanoxane $[\text{R-cp}_6Ti_6O_8]$ (R = H (**11**) or Me (**12**)). Complexes **4–6**, **8**, **9**, **11** and **12** all contain an octahedron of titanium atoms faced by triply bridging oxygen and chlorine in the reported ratio. Molecular orbital calculations showed that a band of 12 non-bonding orbitals may accommodate electrons in excess of those needed for the existence of the Ti_6 skeleton and so the systems can be used in their intact form for storing and releasing electrons. The structures of complexes **4**, **6**, **9** and **12** were determined by single-crystal X-ray diffraction studies.

Keywords: Titanium; Electronic configuration; Titanoxanes; Crystal structure

1. Introduction

Neutral polyoxo aggregates have attracted much attention as molecular precursors of larger metal-oxo fragments, as modeling systems for metal oxides in solution [1–3] and as supports for organometallic fragments [4,5]. The major problem in this field is the absence of a general synthetic methodology for making such species [1] the essential features of which include (i) an organic fragment assuring the solubility in organic solvents, (ii) a very robust skeleton involving bridging donor atoms rather than just weak metal–metal bonds and (iii) a redox behavior which does not affect the molecular skeleton. The two most important methods used so far are the hydrolysis of monomeric precursors [1,6] or the oxidation of very reactive organometallic derivatives [7]. Both methods show poor selectivity and so only very low yields of polyoxo compounds are obtained. In addition, these methods give only species that are in the highest oxidation states and are non-functionalizable.

Details of a novel synthetic methodology [8] involving the reductive coupling of oxochloro titanium(IV) complexes are reported in the present paper. Reduction of compounds belonging to the following cyclopentadienyl-substituted classes of titanium(IV) $[(\text{R-cpTiCl})(\mu_2\text{-O})]_4$ [9] and $[(\text{R-cpTiCl}_2)_2(\mu_2\text{-O})]$ [10] (R = H, Me; R-cp = $\eta^5\text{-RC}_5H_4$) led, depending on the reducing agents and the reaction conditions, to the hexanuclear complexes $[(\text{R-cp})_6Ti_6Cl_{8-n}O_n]$ (n = 4, 6, 8).

[☆] This paper is dedicated to Professor Fausto Calderazzo on the occasion of his 65th birthday, in recognition of his important contributions to organometallic and coordination chemistry.

[*] Corresponding author.

SSDI 0022-328X(94)0011-5

Their synthesis along with a structural and a theoretical study is reported in this paper. Some preliminary results have been communicated [8].

2. Experimental details

2.1. General procedures

All non-hydrolytic procedures were carried out under nitrogen using modified Schlenk-type methods. All reagents and solvents were reagent grade and were dried and degassed by standard procedures before use. IR spectra were recorded for Nujol mulls between KBr plates on a Perkin–Elmer model 883 spectrometer. ^1H and $^{13}C\{^1H\}$ spectra were recorded on a Bruker AC 200 spectrometer. Elemental analyses were carried out with a CHNS-O EA1108 Carlo Erba instrument. Cyclo-tetrakis[μ-oxochloro(R-cyclopentadienyl)titanium-(IV)], $[R\text{-}cpTiCl(\mu_2\text{-}O)]_4$ (R = H, Me, $SiMe_3$) [9,11] and bis[dicloro(cyclopentadienyl)titanium(IV)]oxide, $[R\text{-}cpTiCl_2]_2(\mu_2\text{-}O)]$ (R = H) [10a,11] were prepared by published methods. Distillation of dried solvents, handling of reagents, and syntheses were conducted under purified nitrogen using modified Schlenk glassware and techniques unless otherwise specified.

2.2. Synthesis of $[(R\text{-}cp)_6Ti_6O_6Cl_2]$ (R = H) (4)

2.2.1. Method A: from $[CpTiCl(\mu_2\text{-}O)]_4$ and zinc

To a yellow slurry of $[cpTiCl(\mu_2\text{-}O)]_4$ (15.0 g, 22.8 mmol) in tetrahydrofuran (THF) (300 cm^3) was added zinc dust (6.5 g, 99.4 mmol) containing a catalytic amount of $HgCl_2$. After overnight stirring the royal-blue mixture was transferred to a Soxhlet apparatus and extracted with THF. The crystalline blue solid obtained was filtered off and washed with hexane (100 cm^3) (69%). Found: C, 42.00; H, 4.05; Cl, 8.35. $C_{30}H_{30}Cl_2O_6Ti_6$ calc.: C, 42.65; H, 3.60; Cl, 8.40%. ^1H NMR (pyridine-d_5): δ 6.69 (s, br). ^1H NMR (CD_2Cl_2): δ 6.40 (s, br). $^{13}C\{^1H\}$ NMR: δ 112.1. Chemical ionization (Cl) mass spectrum (NH_3): m/z 516, 358 (M^+).

2.2.2. Method B: from $[cpTiCl(\mu_2\text{-}O)]_4$ and magnesium

By a procedure analogous to method A, the complex $cp_6Ti_6O_6Cl_2$ was prepared from $[CpTiCl(\mu_2\text{-}O)]_4$ (0.99 g, 1.5 mmol) and Mg powder (0.038 g, 1.6 mmol) and $HgCl_2$ (catalytic amount) in THF (100 cm^3). Filtration of the mixture followed by cooling of the filtrate for several days gave the titanium aggregate containing THF of crystallization (32%).

2.2.3. Method C: from $[cpTiCl(\mu_2\text{-}O)]_4$ and sodium

The compound was prepared from $[cpTiCl(\mu_2\text{-}O)]_4$ (0.87 g, 1.3 mmol) and sodium sand (0.063 g, 2.7 mmol) in THF (100 cm^3) using the procedure given in method B. NaCl was filtered off and the filtrate concentrate to half volume. After 36 h a precipitate of the product containing THF of crystallization (31%) was obtained.

2.2.4. Method D: from $[cpTiCl(\mu_2\text{-}O)]_4$ and Bu_3SnH

Tributyltin hydride (1.1 cm^3, 4.0 mmol) was added to a suspension of $[cpTiCl(\mu_2\text{-}O)]_4$ (0.61 g, 0.93 mmol) in toluene (20 cm^3). The mixture was stirred under reflux for 24 h, during which it became royal blue. Upon cooling to room temperature, deep-blue microcrystals precipitated. The product was filtered off, washed with hexane and dried in vacuo (43%).

2.2.5. Method E: from $[cpTiCl(\mu\text{-}O)]_4$ and lithium nitride

By a procedure analogous to method A, the compound was prepared from **1** (1.48 g, 2.25 mmol) and LiN_3 (0.082 g, 2.3 mmol) in THF (60 cm^3). Concentration and cooling of the mixture afforded 0.53 g (33%) of product as a solid containing THF of crystallization.

2.2.6. Method F: from $[cpTiCl(\mu\text{-}O)]_4$ and lithium trisamylborohydride

LS-Selectride (4 cm^3, 4.00 mmol) was added to gently stirred solution of titanoxane **1** (1.31 g, 2.00 mmol) in THF (60 cm^3) at −70°C. The color of the mixture changed from yellow to green and then to deep navy as the stirred mixture was allowed to warm to ambient temperature. Microcrystals of the product (0.11 g, 10%) deposited from the solution when it was set aside.

2.2.7. Method G: from $[cpTiCl_2]_2(\mu_2\text{-}O)$ and Bu_3SnH

To a yellow solution of $[cpTiCl_2]_2(\mu_2\text{-}O)$ (0.49 g, 1.27 mmol) in toluene (50 cm^3) was added tributyltin hydride (0.8 cm^3, 2.9 mmol). After several minutes the mixture became dark blue and, on storage at 2°C, crystals of the product containing 2 modules of toluene of crystallization were obtained (24%). Found: C, 51.15; H, 4.50; Cl, 6.80. $C_{30}H_{30}Cl_2O_6Ti_6 \cdot 2C_7H_8$ calc.: C, 51.30; H, 4.45; Cl, 6.90%.

2.3. Synthesis of $[(Me\text{-}cp)_6Ti_6O_6Cl_2]$ (5)

To a yellow slurry of $[(Me\text{-}cp)TiCl(\mu_2\text{-}O)]_4$ (5.0 g, 7.01 mmol) in toluene (100 cm^3) was added Bu_3SnH (8.16 g, 28.0 mmol). After 24 h stirring under reflux a royal-blue solution was obtained. After storage at −30°C a blue crystalline solid had formed and was collected, washed with ether (50 cm^3) and dried under vacuum for 6 h (80%). Found: C, 46.55; H, 4.55; Cl, 7.35. $C_{36}H_{42}Cl_2O_6Ti_6$ calc.: C, 46.40; H, 4.80; Cl, 7.55%. Proton NMR (pyridine-d_5): δ 6.54 (br, 2H), 6.17 (br, 2H) and 2.58 (br, 3H). Proton NMR (CD_2Cl_2): δ, 6.31 (br, 2H), 5.96 (br, 2H) and 2.50 (br, 3H).

2.4. Synthesis of $[(Me_3Si\text{-}cp)_6Ti_6O_6Cl_2]$ (**6**)

Zn dust (4.12 g, 6.3 mmol), containing a catalytic amount of $HgCl_2$ was added to a solution of $[(Me_3Si\text{-}cp)TiCl(\mu_2\text{-}O)]_4$ (6.91 g, 7.3 mmol) in THF (150 cm^3). After stirring for 2 days a blue mixture was obtained. The solvent was distilled off and the blue residue transferred to a Soxhlet apparatus and extracted with hexane (100 cm^3). A blue crystalline solid was obtained. The suspension was stored at −30°C overnight and filtered while cold. The solid obtained was washed with cold hexane (50 cm^3) and dried under vacuum for 6 hr (72%). Found: C, 45.10; H, 6.15; Cl, 5.75. $C_{48}H_{78}Cl_2O_6Si_6Ti_6$ calc.: C, 44.50; H, 6.30; Cl, 5.55%. IR (Nujol): ν 905 (m, sh); 838 (s, br), 811 (s, sh), 796 (s, sh) cm^{-1}. The NMR spectrum could not be recorded because of the presence of a paramagnetic impurity. The bulk diamagnetism of **6** was proved by a magnetic susceptibility measurement.

2.5. Synthesis of $[cp_6Ti_6O_4Cl_4]$ (**8**)

To a yellow suspension of $[cpTiCl(\mu_2\text{-}O)]_4$ (10.0 g, 1.52 mmol) in THF (250 cm^3) were added aluminium powder (4.0 g, 0.148 mol) and $HgCl_2$ (catalytic amount). Stirring for 3 h resulted in a dark-grey mixture which was transferred to a Soxhlet apparatus and extracted with THF (200 cm^3). A grey microcrystalline solid was obtained and was filtered off, washed with ether (2 × 50 cm^3) and dried under vacuum (48%). Found: C, 40.30; H, 3.70. $C_{30}H_{30}Cl_4O_4Ti_6$ calc.: C, 40.75; H, 3.40%. ESR (2.98 K, THF): g 1.92 (s). ESR (1,1-diphenyl-2-picryl-hydrazyl (DPPH): $g = 1.94$.

2.6. Synthesis of $[(Me\text{-}cp)_6Ti_6O_4Cl_4]$ (**9**)

Aluminium powder (2.53 g, 93.6 mmol) and a catalytic amount of $HgCl_2$ were added to a solution of $[(Me\text{-}cp)TiCl(\mu_2\text{-}O)]_4$ (11.93 g, 16.72 mmol) in THF (250 cm^3). Stirring for 1 day resulted in a dark olive-green mixture. The solvent was evaporated and the residue transferred to a Soxhlet apparatus and extracted with hexane (200 cm^3). Dark-grey microcrystals were produced and were filtered off by filtration, washed with ether (2 × 20 cm^3) and dried under vacuum (59%). Found: C, 40.40; H, 4.40; Cl, 14.50. $C_{36}H_{42}Cl_4O_4Ti_6$ calc.: C, 44.65; H, 4.35; Cl, 14.70%. ESR (2.98 K, THF): $g = 1.91$ (s). ESR (DPPH): $g = 1.94$. Magnetic susceptibility (290 K, BM): μ 2.89 μ_B.

Table 1
Experimental data for the X-ray diffraction studies on crystalline compounds **4**, **6**, **9** and **12**

Parameter (units)	**4**	**6**	**9**	**12**
Formula	$C_{30}H_{30}Cl_2O_6Ti_6 \cdot 2C_7H_8$	$C_{48}H_{78}Cl_2O_6Si_6Ti_6$	$C_{36}H_{42}Cl_4O_4Ti_6$	$C_{36}H_{42}O_8Ti_6$
Crystal system	Monoclinic	Triclinic	Triclinic	Trigonal
Space group	$P2_1/c$	$P\bar{1}$	$P\bar{1}$	$R\bar{3}$
Cell parameters at 295 K [a]				
a (Å)	13.190(3)	13.543(1)	11.486(7)	10.798(3)
b (Å)	12.156(2)	19.584(2)	10.150(7)	10.798(3)
c (Å)	14.665(4)	13.473(1)	9.581(6)	10.798(3)
α (°)	90	92.40	98.79(3)	110.98(2)
β (°)	109.24(2)	114.11(1)	108.96(3)	110.98(2)
γ (°)	90	73.75	108.21(3)	110.98(2)
V ($Å^3$)	2220.9(9)	3120.6(6)	962.4(11)	911.0(7)
Z	2	2	1	1
D_{calc} ($g\ cm^{-3}$)	1.540	1.360	1.670	1.622
Molecular weight	1029.2	1278.0	967.9	890.1
Crystal dimensions (mm)	0.20 × 0.47 × 0.72	0.21 × 0.34 × 0.42	0.37 × 0.40 × 0.55	0.25 × 0.25 × 0.30
Linear absorption coefficient (cm^{-1})	11.84	85.62	14.93	12.90
Radiation	Graphite-mono-	Ni-filtered Cu Kα	Graphite-mono-	Graphite-mono-
Radiation	chromated Mo Kα	(λ = 1.541 78 Å)	chromated Mo Kα	chromated Mo Kα
Radiation	(λ = 0.710 69 Å)		(λ = 0.710 69 Å)	(λ = 0.710 69 Å)
2θ range (°)	6–46	6–120	6–52	6–50
Reflections measured	$\pm h, k, l$	$\pm h, \pm k, l$	$\pm h, \pm k, l$	$\pm h, \pm k, l$
Number of unique total data	3400	9283	3777	3777
Critical intensity for observation	$I > 3\sigma(I)$	$I > 2\sigma(I)$	$I > 3\sigma(I)$	$I > 3\sigma(I)$
Number of unique N_o observed data	1452	4872	2507	846
Number of N_v variables	232	559	226	77
Overdetermination ratio N_o/N_v	6.3	8.7	11.1	11.0
$R = \Sigma \lvert \Delta F \rvert / \Sigma \lvert F_o \rvert$	0.067	0.064	0.039	0.027
$R_w = \Sigma w^{1/2} \lvert \Delta F \rvert / \Sigma w^{1/2} \lvert F_o \rvert$	0.069	0.064	0.040	0.027
Goodness of fit $[\Sigma w \lvert \Delta F \rvert^2 / (N_o - N_v)]^{1/2}$	1.46	2.74	1.53	2.69

[a] Unit-cell parameters were obtained by least-squares analysis of the setting angles of 25–30 carefully centered reflections chosen from diverse regions of reciprocal space.

2.7. Reaction of 7 with Al

To a yellow solution of **7** (1.06 g, 2.77 mmol) in THF (50 cm^3) were added aluminium dust (0.18 g, 6.56 mmol) and HgCl$_2$ (catalytic amount). The solution, which turned green immediately, was stirred overnight. When the resulting deep-green mixture was filtered to remove residual Al, a crystalline mauve solid separated from the filtrate and was filtered off. Successive precipitation of product by concentration or cooling of the reaction solution followed by filtration resulted in a total of 0.84 g (83%) of **10** [12]. IR: ν 3110 (w), 2863 (s), 2828 (s), 1461 (m), 1380 (m), 1020 (m), 825 (s) cm^{-1}.

2.8. Synthesis of [cp$_6$Ti$_6$O$_8$] (11)

A royal-blue mixture of cp$_6$Ti$_6$O$_6$Cl$_2$ (4.56 g, 5.4 mmol) in toluene (150 cm^3) and water (0.2 cm^3, 10.8 mmol) was refluxed for 36 h. The color changed to violet, and bronze-coloured microcrystals separated. The solid was collected, washed with diethyl ether (50 cm^3) and dried overnight (90%). Found: C, 44.70; H 3.75. C$_{30}$H$_{30}$O$_8$Ti$_6$ calc.: C, 44.40; H, 3.85%. Proton NMR (pyridine-d_5): δ 6.39. Proton NMR (CD$_2$Cl$_2$): δ 6.08. IR (Nujol): ν 816 (vs), 791 (vs), 596 (vs), 525 (vs) cm^{-1}.

2.9. Synthesis of [(Me-cp)$_6$Ti$_6$O$_8$] (12)

This compound was prepared by the procedure used for the parent compound cp$_6$Ti$_6$O$_8$. Starting from (Me-cp)$_6$Ti$_6$O$_6$Cl$_2$ (3.0 g, 3.23 mmol), 1.5 g of **12** were obtained (yield, 52%). Proton NMR (pyridine-d_5): δ 6.17 (m, 2H), 6.00 (m, 2H) and 2.39 (s, 3H).

2.10. X-ray crystallography

The crystals selected for study were mounted in glass capillaries and sealed under nitrogen. Crystal data and details associated with data collection are given in Table 1. The reduced cells were obtained with

Table 2
Fractional atomic coordinates ($\times 10^4$) for **6**

Atom	Molecule A			Molecule B		
	x	*y*	*z*	*x*	*y*	*z*
Ti(1)	−798(2)	4860(1)	6155(1)	−1138(2)	497(1)	864(2)
Ti(2)	−1633(1)	5231(1)	3467(1)	−1178(2)	−563(1)	−1182(2)
Ti(3)	40(1)	3861(1)	4692(1)	542(1)	−980(1)	1155(1)
Cl(1)	−2094(3)	6091(2)	4824(2)	−2424(3)	754(2)	−1283(3)
Si(1)	−1833(3)	6133(2)	7995(3)	−3363(3)	2301(2)	489(3)
Si(2)	−4727(3)	5330(2)	2831(3)	−4087(3)	−768(2)	−1674(3)
Si(3)	2043(3)	2015(2)	6045(3)	2575(3)	−1541(2)	4186(2)
O(1)	−1325(5)	4587(3)	4703(4)	−1113(5)	−448(3)	297(5)
O(2)	635(5)	4070(4)	6334(6)	508(5)	−32(3)	1752(6)
O(3)	176(5)	5448(3)	6451(5)	−460(5)	1055(4)	324(5)
C(1)	−1582(8)	5232(3)	7448(7)	−2524(7)	1400(4)	1220(6)
C(2)	−589(8)	4657(4)	7965(7)	−2886(7)	774(4)	1057(6)
C(3)	−770(7)	4036(4)	7425(6)	−2088(7)	250(3)	1915(6)
C(4)	−1875(8)	4227(4)	6573(7)	−1232(7)	552(4)	2608(6)
C(5)	−2377(8)	4967(4)	6587(7)	−1502(7)	1263(4)	2179(6)
C(6)	−3576(6)	5350(4)	2415(6)	−2793(6)	−987(4)	−1977(7)
C(7)	−2949(6)	4763(4)	2057(5)	−1838(6)	−1588(4)	−1473(7)
C(8)	−2357(5)	5029(4)	1577(6)	−1130(6)	−1659(4)	−2034(7)
C(9)	−2618(6)	5780(4)	1639(6)	−1647(6)	−1101(4)	−2884(7)
C(10)	−3372(6)	5978(4)	2157(6)	−2675(6)	−686(4)	−2849(7)
C(11)	707(4)	2598(3)	4989(5)	1481(5)	−1693(4)	2848(5)
C(12)	508(4)	2783(4)	3902(5)	1718(5)	−2130(4)	2058(5)
C(13)	−668(4)	3109(4)	3313(5)	686(5)	−2228(4)	1286(5)
C(14)	−1197(4)	3125(4)	4036(5)	−188(5)	−1852(4)	1599(5)
C(15)	−347(4)	2809(4)	5071(5)	303(5)	−1521(4)	2565(5)
C(16)	−2902(12)	6825(6)	6915(10)	−2406(11)	2759(6)	344(10)
C(17)	−2367(13)	6080(9)	9060(13)	−4007(13)	2824(8)	1384(13)
C(18)	−445(12)	6328(6)	8640(10)	−4425(12)	2208(8)	−843(13)
C(19)	−4324(11)	4503(8)	3648(11)	−4876(12)	178(8)	−2036(15)
C(20)	−5050(1)	6098(7)	3563(13)	−3661(11)	−973(9)	−225(12)
C(21)	−6010(11)	5364(9)	1553(13)	−5001(12)	−1295(9)	−2509(13)
C(22)	1842(11)	1107(6)	5954(12)	3035(12)	−2341(8)	5171(11)
C(23)	3251(10)	2028(8)	5762(12)	3816(11)	−1461(9)	4032(11)
C(24)	2204(11)	2318(8)	7391(10)	1945(13)	−733(9)	4693(12)

Table 3
Fractional atomic coordinates ($\times 10^4$) for **4**

Atom	x	y	z	Atom	x	y	z
Ti(1)	4801(2)	1845(2)	-140(2)	C(12)	2224(13)	-647(13)	1031(14)
Ti(2)	3706(2)	-376(2)	-1421(2)	C(13)	2865(13)	63(16)	1770(11)
Ti(3)	3546(2)	166(2)	471(2)	C(14)	2701(14)	1110(14)	1437(13)
C(1)	4777(3)	1312(3)	-1840(3)	C(15)	2027(14)	1133(15)	524(14)
O(1)	3484(6)	914(7)	-684(5)	C(1S)	-20(17)	3096(17)	2103(15)
O(2)	4826(6)	911(6)	1062(5)	C(2S)	-579(17)	3936(17)	2379(15)
O(3)	6233(7)	1105(7)	169(6)	C(3S)	-1237(17)	4642(17)	1685(15)
C(1)	3797(13)	3487(11)	-656(13)	C(4S)	-1338(17)	4508(17)	714(15)
C(2)	3994(21)	3353(12)	327(18)	C(5S)	-780(17)	3668(17)	438(15)
C(3)	5165(20)	3444(12)	772(11)	C(6S)	-121(17)	2962(17)	1132(15)
C(4)	5619(13)	3622(11)	57(14)	C(7S)	721(34)	2443(41)	2887(30)
C(5)	4734(16)	3652(10)	-813(11)	C(8S)	-168(29)	3237(31)	2191(18)
C(6)	1902(11)	-779(19)	-2282(12)	C(9S)	172(29)	2568(31)	1575(18)
C(7)	2285(15)	-18(16)	-2814(12)	C(10S)	-155(29)	2796(31)	588(18)
C(8)	3059(13)	-530(14)	-3124(9)	C(11S)	-823(29)	3694(31)	217(18)
C(9)	3192(11)	-1591(12)	-2774(10)	C(12S)	-1163(29)	4363(31)	833(18)
C(10)	2491(14)	-1721(14)	-2257(11)	C(13S)	-836(29)	4134(31)	1820(18)
C(11)	1665(11)	53(17)	244(12)	C(14S)	125(43)	3185(50)	3157(41)

the use of TRACER [13]. Data were collected at room temperature (295 K) on a single-crystal four-circle diffractometer. For intensities and background the three-point technique was used for **4**, **9** and **12**, while individual reflection profiles were analyzed for **6** [14]. The structure amplitudes were obtained after the usual Lorentz and polarization corrections [15] and the absolute scale was established by the Wilson [16] method. The crystal quality was tested by ψ scans showing that crystal absorption effects could be neglected for complexes **4**, **9** and **12**. Data for **6** were corrected for absorption [17], with maximum and minimum corrections of 1.056–1.219. The function minimized during the full-matrix least-squares refinement was $\Sigma w \mid \Delta F \mid^2$. Weights were applied according to $w = k/[\sigma^2(F_o) + \mid g \mid F_o^2]$ based on counting statistics. Anomalous scattering corrections were included in all structure factor calculations [18b]. Scattering factors for neutral atoms were taken from [18a] for non-hydrogen atoms and from [19] for H. Among the small-angle reflections no correction for secondary extinction was deemed necessary.

Solutions and refinements were based on the observed reflections. The structures were solved by the heavy-atom method starting from a three-dimensional Patterson map. Refinement was first isotropically and then anisotropically for non-H atoms carried out by the full-matrix least-squares method for **4**, **9** and **12**, and by the blocked (two blocks) full-matrix least-squares method for **6**. The toluene solvent molecules in **4** were isotropically refined. All the hydrogen atoms but those associated to the toluene molecules, which were ignored, were introduced in calculations as fixed contributors with isotropic U values fixed at 0.08 Å^2. Most of the hydrogen atoms were located from difference maps; some others were put in geometrically calculated positions. Excluding **9**, all the Cp rings and the methyl carbon atoms are affected by severe thermal motion, as often happens in a situation such as this. During the refinement of **6** the Cp rings were treated as regular

Table 4
Fractional atomic coordinates ($\times 10^4$) for **9**

Atom	x	y	z	Atom	x	y	z
Ti(1)	1939(1)	4858(1)	1658(1)	C(7)	3425(5)	8769(5)	-35(6)
Ti(2)	1750(1)	6481(1)	-510(1)	C(8)	4032(5)	7790(6)	239(7)
Ti(3)	-331(1)	2869(1)	-2029(1)	C(9)	3614(6)	6736(6)	-1181(8)
Cl(1)	-398(1)	5027(1)	-3141(1)	C(10)	2736(6)	7075(6)	-2310(7)
Cl(2)	-60(1)	2239(1)	538(1)	C(11)	2596(6)	8312(6)	-1639(7)
O(1)	1740(3)	6708(3)	1561(3)	C(12)	3624(7)	10048(6)	1131(8)
O(2)	1360(3)	4447(3)	-584(3)	C(13)	786(6)	1716(5)	-3263(6)
C(1)	4131(5)	6079(6)	3675(6)	C(14)	93(6)	755(6)	-2636(6)
C(2)	3423(6)	5047(7)	4226(7)	C(15)	-1289(6)	440(5)	-3398(7)
C(3)	3019(6)	3680(7)	3259(7)	C(16)	-1418(6)	1233(6)	-4478(6)
C(4)	3520(6)	3849(6)	2116(7)	C(17)	-135(6)	2010(6)	-4383(6)
C(5)	4200(5)	5331(6)	2353(6)	C(18)	2287(7)	2354(8)	-2770(9)
C(6)	4694(7)	7690(7)	4391(8)				

Table 5
Fractional atomic coordinates ($\times 10^4$) for **12**

Atom	*x*	*y*	*z*	Atom	*x*	*y*	*z*
Ti(1)	149(1)	1424(1)	1985(1)	C(3)	−57(6)	3577(5)	3426(4)
O(1)	2241(3)	2241(3)	2241(3)	C(4)	1499(5)	3979(4)	4374(4)
O(2)	−2050(2)	−453(2)	262(2)	C(5)	1392(5)	2888(5)	4791(4)
C(1)	−174(5)	1818(4)	4130(4)	C(6)	−544(9)	4418(7)	2702(6)
C(2)	−1085(4)	2225(5)	3281(4)				

pentagons. The final difference maps showed no unusual feature, with no significant peak above the general background.

Final atomic coordinates are listed in Tables 2–5 for non-H atoms, and selected bond distances and angles in Table 6. Complete lists of bond lengths and angles, and tables of hydrogen atom coordinates and thermal parameters have been deposited at the Cambridge Crystallographic Data Centre.

3. Computational details

Calculations were performed by using the extended Hückel approximation [20]. The following orbitals were used: 3d, 4s and 4p for titanium; 2s and 2p for carbon and oxygen; 3s and 3p for chlorine; 1s for hydrogen. The parameters for the orbitals, taken from [21], can be obtained from the authors.

The geometries of the $cp_6Ti_6O_8$, $cp_6Ti_6O_6Cl_2$, and $cp_6Ti_6O_4Cl_4$ clusters were taken from this work and [22]. Minor deviations in equivalent distances and angles were averaged to obtain a structure with the highest symmetry possible. A standard geometry was used for the cyclopentadienyl rings: C–C, 1.4 Å; C–H, 0.91 Å; C–C–C, 108°; C–C–H, 126°. The geometries of the $cp_6Ti_6O_2Cl_6$ and $cp_6Ti_6Cl_8$ clusters were deduced from those of the other clusters of the series. For $cp_6Ti_6O_2Cl_6$ we have assumed an elongated octahedral geometry with Ti–Ti distances of 3.4 Å. The effective symmetries are O_h for $cp_6Ti_6O_8$ and $cp_6Ti_6Cl_8$, D_{2h} for $cp_6Ti_6O_4Cl_4$, and C_{2h} for $cp_6Ti_6O_6Cl_2$ and $cp_6Ti_6O_2Cl_6$. The presence of the static cyclopentadienyl rings reduces in the calculations the symmetry to at best D_{3d} for the octahedral clusters and C_{2h} for the others. In the reported results, however, we have used the symmetry labels of the idealized symmetries.

4. Results and discussion

4.1. Synthesis and properties of hexanuclear titanoxanes

Reduction of oxo-chloro complexes had no precedent when we originally decided to reduce oxo-chloro compounds of titanium(IV) [8]. Indeed, only recently have a few applications of this method been published [23,24]. We expected to obtain from such a reaction reactive reduced unsaturated fragments which would collapse, eventually to form an aggregate. The choice of the reducing agent was mainly based on its affinity for Cl or O, these being probable leaving groups, or on the reducing mechanism. The choice of the starting material $[(R\text{-}cpTiCl)_4(\mu\text{-}O)_4]$($cp = \eta^5\text{-}RC_5H_4$; R = H, Me or $SiMe_3$) was mainly based on their ease of synthesis by the hydrolysis of ($R\text{-}cpTiCl_3$) [11].

The reduction of the tetrachloro titanoxanes **1–3** was first carried out with zinc activated by $HgCl_2$. The following reaction gave royal-blue crystals of **4–6**:

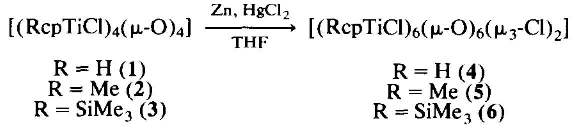

$$[(RcpTiCl)_4(\mu\text{-}O)_4] \xrightarrow[THF]{Zn,\ HgCl_2} [(RcpTiCl)_6(\mu\text{-}O)_6(\mu_3\text{-}Cl)_2] \quad (1)$$

R = H (**1**)
R = Me (**2**)
R = SiMe$_3$ (**3**)

R = H (**4**)
R = Me (**5**)
R = SiMe$_3$ (**6**)

The reductive coupling reaction on **1** was successfully carried out with a variety of reducing agents. Among them was LiN_3, which is not normally regarded as a reductant. However, there is a report of its use for reducing titanium(IV) compounds [25].

After successful utilization of several heterogeneous reagents (Zn, Mg or Na) we investigated synthesis of the low valency aggregates via homogeneous reductions typically used for organic compounds. Two such reagents differing in their reduction mechanisms were selected: lithium trisamyl borohydride and tributyltin. Whilst the former reductant is ionic in character, reductions employing $^nBu_3SnH$ usually involve a radical mechanism.

The reaction with lithium trisamyl borohydride (LS-selectride) gave a particularly poor yield compared with those from the other reducing agents. Furthermore, there is a non-selective generation of other reducing species concurrent with the intermediate building block leading to **4**.

The generation of an organotin radical from $^nBu_3SnH$ is often used to abstract a halogen atom from an organic halide to afford a carbon-centered radical species [26]. We envisaged that the analogous reaction with a titanium(IV) halide complex would produce a titanium(III) center, a typical inorganic (d^1) free radical. When a mixture of **1** and $^nBu_3SnH$ in toluene was heated for 24 h, the typical royal-blue

Table 6
Selected interatomic distances (Å) and angles (°) in **4**, **6**, **9**, **12**

9		**12**	
Ti(1)–Cp(1)	2.045(7)	Ti(1)–Cp(1)	2.083(4)
Ti(2)–Cp(2)	2.054(7)		
Ti(3)–Cp(3)	2.050(7)		
Ti(1)–Ti(2)	2.837(2)	Ti(1)–Ti′	2.899(1)
Ti(1)–Ti(3)	2.450(3)	Ti(1)–Ti″	2.899(1)
Ti(2)–Ti(3)	3.451(3)	Ti(1)–Ti$^{\mathrm{iii}}$	2.896(2)
Ti(2)–Ti(3′)	3.430(2)	Ti(1)–Ti$^{\mathrm{iv}}$	2.896(2)
Ti(1)–Ti(2′)	3.732(2)		
Ti(1)–Ti(3′)	3.421(2)		
O(1)–Ti(1)	1.973(4)	O(1)–Ti(1)	1.976(3)
O(1)–Ti(2)	1.966(4)	O(1)–Ti′	1.976(3)
O(1)–Ti(3′)	1.963(4)	O(1)–Ti″	1.976(3)
O(2)–Ti(1)	1.964(4)	O(2)–Ti(1)	1.974(2)
O(2)–Ti(2)	1.956(4)	O(2)–Ti$^{\mathrm{iii}}$	1.982(3)
O(2)–Ti(3)	1.971(3)	O(2)–Ti$^{\mathrm{iv}}$	1.970(3)
Cl(1)–Ti(1′)	2.623(2)		
Cl(1)–Ti(2)	2.677(2)		
Cl(1)–Ti(3)	2.589(2)		
Cl(2)–Ti(1)	2.684(2)		
Cl(2)–Ti(2′)	2.647(2)		
Cl(2)–Ti(3)	2.581(2)		

4		**6**	
		Molecule A	Molecule B
Ti(1)–Cp(1)	2.040(14)	2.055(12)	2.068(10)
Ti(2)–Cp(2)	2.031(14)	2.053(6)	2.058(8)
Ti(2)–Cp(3)	2.052(20)	2.048(8)	2.067(8)
Ti(1)–Ti(2)	3.334(3)	3.367(3)	3.372(3)
Ti(1)–Ti(3)	2.947(4)	3.043(3)	3.062(2)
Ti(2)–Ti(3)	2.927(4)	2.995(2)	3.027(2)
Ti(2)–Ti(3′)	3.438(3)	3.373(3)	3.359(3)
Ti(1)–Ti(2′)	3.055(3)	3.073(3)	3.026(3)
Ti(1)–Ti(3′)	3.416(4)	3.358(3)	3.374(3)
O(1)–Ti(1)	2.006(8)	1.899(6)	1.970(7)
O(1)–Ti(2)	1.980(9)	1.963(7)	1.965(7)
O(1)–Ti(3)	1.901(9)	1.996(6)	2.030(6)
O(2)–Ti(1)	2.088(8)	2.047(7)	2.026(5)
O(2)–Ti(2′)	1.944(8)	2.117(8)	2.001(9)
O(2)–Ti(3)	1.860(8)	2.089(9)	1.988(7)
Cl(1)–Ti(1)	2.568(5)	2.745(3)	2.678(4)
Cl(1)–Ti(2)	2.675(5)	2.579(4)	2.631(4)
Cl(1)–Ti(3′)	3.037(4)	2.614(4)	2.643(4)
O(3)–Ti(1)	2.005(9)	1.900(8)	1.933(9)
O(3)–Ti(2)	2.017(9)	2.010(6)	1.997(6)
O(3)–Ti(3′)	1.880(9)	1.968(7)	1.952(7)

Cp1, Cp2, Cp3 refer to the centroids of the cyclopentadienyl rings.
′, $-x$, $1-y$, $-z$ (**9**); z, x, y (**12**); $1-x$, $-y-z$ (**4**); $-x$, $1-y$, $1-z$ (**6**, molecule A); $-x$, $-y$, $-z$ (molecule B); ″, y, z, x (**12**); $^{\mathrm{iii}}=-z$, $-x$, $-y$ (**12**); $^{\mathrm{iv}}=-y$, $-z$, $-x$ (**12**); $^{\mathrm{v}}=-x$, $-y$, $-z$ (**12**).

colour of **4** appeared. When the solution was allowed to cool to room temperature, crystals of **4** were obtained with a good yield. The soluble nature of both the reactant $^{n}\mathrm{Bu_3SnH}$ and the byproduct $^{n}\mathrm{Bu_3SnCl}$ means that this method is much cleaner than the previous heterogeneous reactions.

$$\underset{\mathbf{1}}{[(\mathrm{cpTiCl})_4(\mu\text{-O})_4]} \xrightarrow[-\mathrm{Bu_3SnCl},\ -\mathrm{H_2}]{\mathrm{Bu_3SnH}\ (\text{toluene, } 82^\circ\mathrm{C})} \mathbf{4} \qquad (2)$$

Reductive coupling of the μ-oxo dimer **7** with $^{n}\mathrm{Bu_3SnH}$ gives the same product **4**, but the reaction is much faster. The major byproduct is the well-known $[\mathrm{cpTiCl_2}]$ complex [12]. The dinuclear oxo-complex **7** gives **4** together with other species, but its use was not pursued because of the low yields and the isolation in many of these reactions of a mixture of crystalline solids.

$$\underset{\mathbf{7}}{[(\mathrm{cpTiCl_2})_2(\mu\text{-O})_2]} \xrightarrow[-\mathrm{Bu_3SnCl},\ -\mathrm{H_2}]{\mathrm{Bu_3SnH}\ (\text{toluene})} \mathbf{4} \qquad (3)$$

Compounds **4**–**6** were soluble in pyridine, less so in toluene and THF, and only sparingly in diethyl ether. The solubility is higher for the cp-substituted derivatives. They are thermally stable but decompose rapidly upon exposure to air in the solid state and almost immediately in solution to give eventually yellow titanium(IV) products. They are diamagnetic, although they should be regarded formally as containing four titanium(III) and two titanium(IV) metal centers. The ^{1}H NMR spectra of **4**–**6** showed broadened signals for the organic ligand protons at typical chemical shifts. Diagnostic IR band identifiable with certainty were the C–H stretching vibrations around 3090 cm^{-1}, and the C–C stretching vibrations at 1460 cm^{-1}. The mass spectra showed the $\mathrm{M^+}$ peaks, with the expected chlorine isotope pattern.

For all the reducing agents so far explored we must emphasize that the use of the reported stoichiometry is essential. A major difference encountered between the various reducing agents is the yield of the hexanuclear complex. This arises from the separation of the desired product from other compounds of low solubility. Consequently, the yield was particularly good in the case of $^{n}\mathrm{Bu_3SnH}$ for the reasons described above. In addition, the generation of the reactive fragment leading to the hexanuclear species may parallel the formation of other fragments leading to different products, again depending upon the nature of the reducing agent.

A significant example of the dependence of the reduced species on the nature of the reducing agent was obtained when aluminum metal was used. The reaction was carried out with **1** and **2** in THF using activated Al metal.

$$\underset{\substack{\mathrm{R=H}\ (\mathbf{1})\\ \mathrm{R=Me}\ (\mathbf{2})}}{[(\mathrm{RcpTiCl})_4(\mu_2\text{-O})_4]} \xrightarrow[\mathrm{THF}]{\mathrm{Al,\ HgCl_2}} \underset{\substack{\mathrm{R=H}\ (\mathbf{8})\\ \mathrm{R=Me}\ (\mathbf{9})}}{[(\mathrm{RcpTi})_6(\mu_3\text{-O})_4(\mu_3\text{-Cl})_4]} \qquad (4)$$

Complexes **8** and **9** separated out from either a concentrated THF solution in the case of **8**, or from a cold THF-Et_2O mixture in the case of **9**. Both thermally stable complexes are soluble in THF, less so in toluene and sparingly in diethyl ether. Solubility, as in the case of the unsubstituted and substituted analogs **4–6**, was again higher for the substituted compound. Upon exposure to air, **8** and **9** decomposed rapidly in the solid state and almost instantaneously in solution, finally giving yellow Ti(IV) products. Qualitatively, the rate of decomposition appeared to be faster for the unsubstituted compound. Complexes **8** and **9** contain two unpaired electrons according to magnetic susceptibility measurements (2.89 μ_B at 290 K) and, as expected from the fast relaxation times in paramagnetic species, NMR spectra showed very broad signals. Diagnostic IR bands were observed at 3105 and 3090 cm^{-1} (C–H stretching), and 1458 and 1455 cm^{-1} (C–C stretching) for **8** and **9** respectively. In the mass spectrum of aggregate **9** the molecular ion M^+ was found at $m/z = 572$ with the characteristic chlorine isotope pattern. The formation of **8** and **9** instead of **4** and **5** is understandable on the basis of the oxophilicity of aluminum, which thus prefers to reduce by the removal of an oxygen atom rather than a chloride. Another example of this is the deoxygenation of **7** by Al to give **10** [12]:

$$\underset{\mathbf{7}}{[(cpTiCl_2)(\mu_2\text{-}O)]} \xrightarrow[Al-HgCl_2]{THF} \underset{\mathbf{10}}{[(cpTiCl_2)(THF)_{1.5}]} \qquad (5)$$

The isolation of **8** and **9** in the case of aluminum may be related to the change in the redox potential on going from Zn to Al but, under the reaction conditions used, such a parameter is hard to define.

It was observed that during work-up of the dichloro aggregates **4** and **5** a precipitate of a deeply colored material, with different crystallinity, stability and spectral characteristics from those of the main products was obtained. This was initially believed to be a second product of the reduction reaction. However, an NMR experiment showed that the progressive disappearance of **4** and **5** in pyridine-d_5 solution containing traces of moisture resulted in the concomitant formation of these secondary products. They were subsequently identified as **11** [27] and **12**. The oxo complexes were prepared by controlled hydrolyses of the respective complexes **4** and **5** in refluxing toluene containing a few drops of deionized H_2O:

$$[(RcpTi)_6(\mu_3\text{-}O)_6(\mu_3\text{-}Cl)_2] \xrightarrow[toluene]{H_2O} [(RcpTi)_6(\mu_3\text{-}O)_8] + 2HCl + H_2$$

R = H (**4**) R = H (**11**)
R = Me (**5**) R = Me (**12**)

(6)

Reaction (6) involves not only hydrolysis of the Ti–Cl bonds but also oxidation of the metallic core by two electrons. Although the formation of H_2 is expected, it was never been detected owing to the vigorous conditions under which reaction (6) is carried out. The compounds were obtained as either finely crystalline violet solids or as large bronze-colored parallelepiped crystals, on which it was possible to carry out a single-crystal X-ray diffraction study of aggregate **12**. Hydrolyses of the tetrachloro aggregates **8** and **9** also appeared to give the oxo derivatives but not cleanly. The solubilities of **11** and **12** in various organic solvents were slightly lower than those of the dichlorinated compounds. They were also thermally stable. Both in the crystalline form and in solution, however, the oxo derivatives were significantly more stable towards oxidation and hydrolysis by air than were the chlorinated starting materials. This could be expected from the fact that, formally, the dichloro compounds contained four electron-rich Ti(III) ions whereas there are only two in the oxo derivatives.

Complexes **11** and **12** are diamagnetic. Their NMR spectra showed sharp peaks for the organic ligand protons in contrast with the broadened signals recorded for the chlorinated precursors and were moved upfield by 0.2–0.3 ppm. The C–H stretching frequencies in the IR were recorded as weak doublet peaks at 3110 and 3090 cm^{-1} for **11** and **12** respectively, while the C–C stretching bands were both observed at 1460 cm^{-1}. The strong band at 598 cm^{-1} in both spectra has been assigned as one of the allowed T_{1u} Ti–O vibrations. Compound **11** was reported as a secondary low yield product from the hydrogenation of carbon monoxide bonded to titanium in $cp_2Ti(CO)_2$ [27]. The water formed during the reaction, as was proved subsequently, is responsible for hydrolyzing the dicarbonyl to the titanoxane (**11**) [28].

4.2. Structures of the hexanuclear titanoxanes

The structures of **4**, **6**, **9** and **12** are shown in Figs. 1, 2, 3 and 4 respectively. Selected bond distances and angles related to the metallic core are listed in Tables 6 and 7. The four compounds were found to be discrete hexanuclear molecules in the crystalline state. The general structure feature is an octahedral-like metal skeleton defined by six Rcp-capped titanium ions arranged centrosymmetrically. The ions are held together by triply bridging oxygen or chlorine atoms located above each of the eight triangular faces of the octahedron. Penta-coordination geometry around titanium is, with some variation, of square pyramidal type having the basal plane defined by the heteroatoms O, Cl and the apex by a ring ligand centroid. There are no strong interactions between the titanium ions (shortest Ti ··· Ti distance is 2.838 Å) and the Ti–Cl and Ti–O separations indicated single bonds between metal units and bridging groups. Rcp-Ti distances fall in the nar-

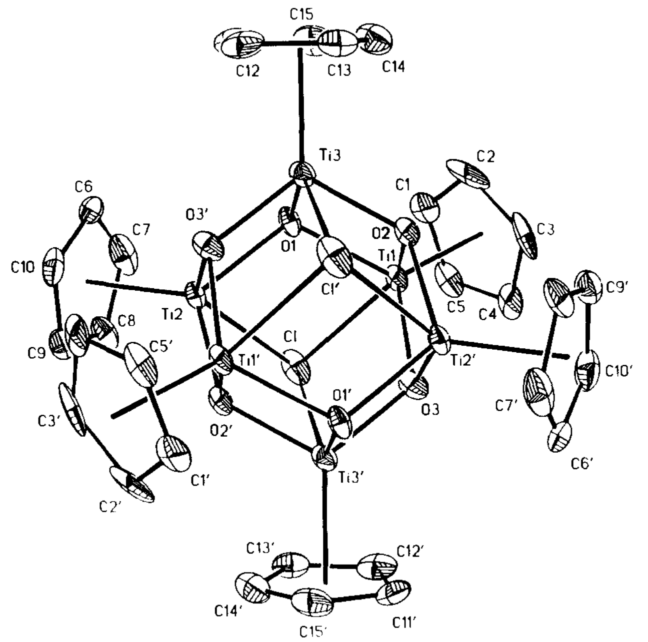

Fig. 1. An ORTEP drawing for **4** (30% probability ellipsoids).

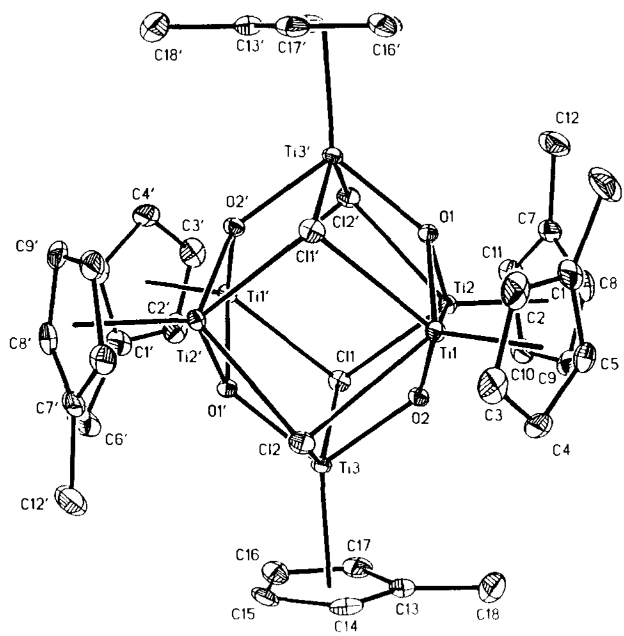

Fig. 3. An ORTEP drawing for **9** (30% probability ellipsoids).

row range 2.031–2.080 Å, almost unchanged from those in the starting titanoxanes [10].

The structural make-up of **4** differs from that of the highly symmetric (O_h) [(cpTi)$_6$(μ_3-O)$_8$] (**11**) [27] in which two oxygen bridges on opposite parallel faces of the octahedron are replaced by chlorine atoms (Fig. 1). Face-bridging trihapto chlorine ligands were previously unknown in titanium chemistry. A significant elongation of the metallic octahedral cage results from this ligand change, as revealed by the increase in the average Ti · · · Ti separation from 2.891 Å in the oxo complex **11** to 3.069 Å in **4**. Each of the six titanium centers has the same atomic environment, with a square pyramid coordination geometry defined by three oxygen atoms and a chlorine atom in the basal plane and the centroid of the cyclopentadienyl ligand at the apex. Displacements of the metal ions from the basal plane are 0.963(3) Å, 0.972(3) Å and 0.947(3) Å for Ti(1), Ti(2) and Ti(3) respectively.

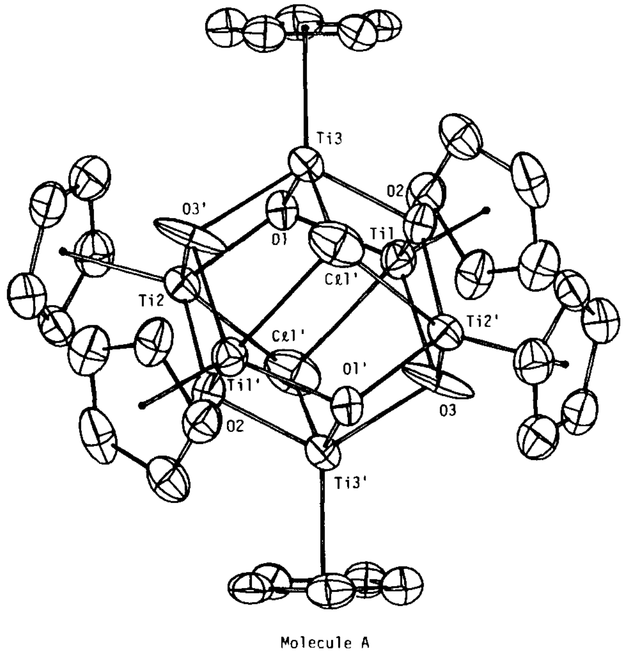

Fig. 2. An ORTEP drawing for **6** (molecule A, 30% probability ellipsoids). The SiMe$_3$ groups have been omitted for clarity.

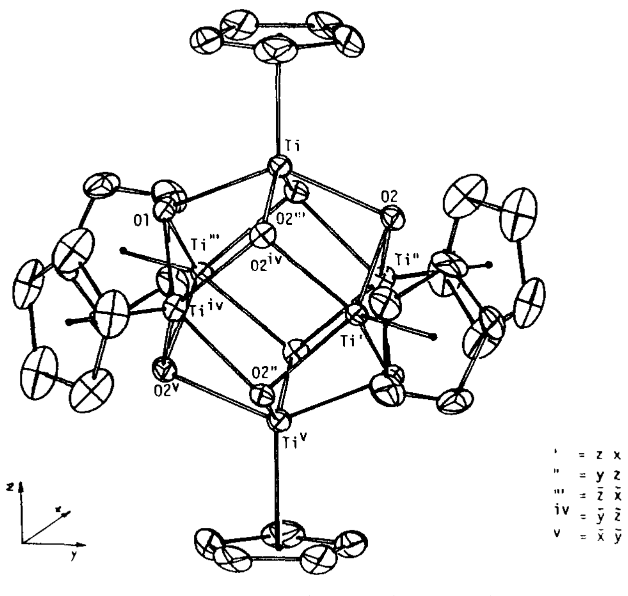

Fig. 4. An ORTEP drawing for **12** (30% probability ellipsoids). The Me carbon atoms have been omitted for clarity.

Table 7
Relevant parameters for the coordination polyhedra

		Value for the following complexes				
		4	6	9		12
				Molecule A	Molecule B	
Displacement [a] (Å)	Ti(1)	1.020(2)	0.966(2)	0.946(2)	0.966(2)	0.759(1)
	Ti(2)	1.025(2)	0.968(2)	0.952(2)	0.949(2)	–
	Ti(3)	0.986(2)	0.950(3)	0.940(2)	0.964(2)	–
Angle [b] (°)	Ti(1)	4.1(2)	2.6(5)	4.8(3)	4.4	0.9(2)
	Ti(2)	4.0(2)	2.5(4)	5.4(3)	5.4	–
	Ti(3)	4.9(2)	2.2(5)	3.1(2)	3.5	–
Angle [c] (°)	Ti(1)	2.2(2)	1.3(4)	4.8(3)	3.9(3)	5.4(1)
	Ti(2)	2.5(2)	1.3(4)	4.8(2)	4.4(3)	–
	Ti(3)	1.6(2)	2.4(6)	2.8(2)	2.9(3)	–

[a] Displacements of the titanium atoms from the mean basal plane.

[b] Dihedral angles formed by the Ti–Cp direction and the normal to the basal plane.

[c] Dihedral angles formed by the basal plane and the Cp ring.

Despite the small asymmetry in the μ_3-O functionality (e.g. O(1)–Ti(1) equal to 2.006(8) Å, O(1)–Ti(2) equal to 1.980(9) Å and O(1)–Ti(3) equal to 1.900(8) Å) the combined average (1.964 Å) closely resembles those reported for the oxo derivative **11** (1.973 Å) [27] and the titanoxane **1** (1.965 Å) [10c]. These values are in good agreement with an earlier estimate of 2.0 Å for the single Ti–O bond [10b] and reflect a reduction in π bonding between filled p_p orbitals on oxygen and vacant d_p orbitals on the titanium atoms which results in the partial double-bond character (1.8 Å) present in the starting titanoxanes and related oxo-bridged Ti(IV) complexes [29]. The range of bond angles at oxygen was large (96.4(1)–129.3(5)°) because there are two structurally distinct types. Smaller values ranging from 96.4(3)° to 98.9(4)° were observed in bridges opposite another oxygen ligand (e.g. Ti(1)–O(2)–Ti(3)) while the larger angles, ranging from 113.6(4)° to 129.3(4)° (e.g. Ti(1)–O(1)–Ti(2)), were found at oxygen atoms facing chlorine bridges. Titanium–chlorine distances for the μ_3-Cl ligand showed significant internal variation (e.g. Cl–Ti(1) equal to 2.567(5) Å, Cl–Ti(2) equal to 2.675(5) Å, Cl–Ti(3) and equal to 3.037(4) Å) and were uniformly higher than the approximate value of 2.3 Å observed for either the Ti(IV) titanoxane **1** or the Ti(III) complex cpTiCl$_2$ **5** [12b]. Bond angles at chlorine atoms ranged from 73.7(1)° to 79.0(1)°. The three metal-to-ring centroid distances were all 2.04 Å within experimental error, thus excluding a localized oxidation state description.

Interest in the X-ray study of **6** (Fig. 2) lay in determining what effect, if any, the SiMe$_3$ substituent on the cp ring had on the aggregate structure. Fig. 2 shows only one (A) of the two independent molecules A and B present in the asymmetric unit, but the substitution had almost no effect on the oxo-aggregate structure in the solid state (Tables 6 and 7). The substitution had a major influence only on the solubility of the compound.

The metallic octahedral trame of complex **9** (Fig. 3), composed of six formally Ti(III) atoms, shows a significant elongation from the regular octahedral shape. This distortion is observed along the z axis lying at the intersection of the plane containing the four μ_3-Cl groups (e.g. the y–z plane in a cartesian coordinate system) with the plane containing the four μ_3-O$_3$ bridges (x–z) (Scheme 1).

The four basal Ti(1), Ti(2), Ti(1′) and Ti(2′) corners of the octahedron are located on the mutually perpendicular (x–y) plane (see Scheme 1). If the ring ligands are neglected, then each of these structural planes becomes a symmetry mirror plane of the centrosymmetric molecule.

As a result of the octahedral elongation the six titanium centers are differentiated into two axial and four equatorial environments (Ti(3), Ti(3′) and Ti(1), Ti(1′), Ti(2), Ti(2′) respectively). In the equatorial rectangle the Ti$_{eq}$ ··· Ti$_{eq}$ separations average 3.284 Å, while the eight Ti$_{eq}$ ··· Ti$_{ax}$ distances are close to

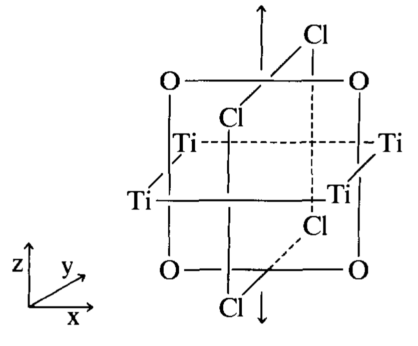

Scheme 1.

3.438 Å, and the $Ti_{ax} \cdots Ti_{ax}$ distance is 5.030 Å. Displacements from the square pyramidal geometry toward a trigonal bipyramid was observed around Ti(3′) (Fig. 3). The pyramid equatorial plane is defined by the two apical Cl(1′) and Cl(2′) groups situated at 138.8(1)° about the central ion. No other O–Ti–O or Cl–Ti–O angle in the molecule was larger than 125.5(1)°.

All the $Ti \cdots O$ bond lengths are virtually equal, within the standard deviations, to the average value of 1.965 Å, thus indicating symmetric μ_3-O bridges with Ti–O single bonds. The value agrees well with the 1.97 Å estimate for the cpTi(III)–O contact predicted by Bottomley et al. [30]. Bond angles at oxygen atoms are, as in **4** and **6**, of two types: small when facing another Ti-O-Ti bridge (Ti(1)–O(1)–Ti(2), 92.2(2)°; Ti–O(2)–Ti(2), 92.8 (2)°) and larger when facing a Ti–Cl–Ti bridge (Ti(1)–O(1)–Ti(3′), 121.7(2)°; range, 120.8(2)–122.9(2)°).

The μ_3-chloro functionality is also nearly symmetric (Ti–Cl separation range, 2.589(2)–2.684(2) Å) with an average bond length of 2.633 Å. This is longer than the terminal Ti(III)–Cl bond length of 2.347 Å in $[cpTiCl_2(thf)_{1.5}]$ **(5)** [12b]. Bond angles around chlorine can also be classified into two types depending on the opposite bridging element, although the effect is much less pronounced than for oxygens. The Ti–Cl–Ti bridges facing oxygen atoms (e.g. Ti(1)–Cl(2)–Ti(2′) are slightly large (range, 88.9(1)°–92.2(2)°; average, 90.2(3)°). The six metal-to-ring centroid distances average 2.051 Å, showing no significant change from that of titanoxane **2** (2.038 Å). All the methyl groups are arranged in the same (arbitrary) sense, possibly to avoid steric repulsions.

The Ti_6O_8 cage in **12** (Fig. 4) displays the same high O_h symmetry as that in $[(cpTi)_6(\mu_3\text{-}O)_8]$ **(11)** [27]. Its μ_3-O bridges and interatomic separations are also essentially equal to those in the unsubstituted compound (Tables 6 and 7). The Ti–O bond distances are close to those in the other hexamers **4** and **6**, while the most important difference is found in the Ti–Ti separations which become very short in the fully oxygenated form (Table 6). A comparison of interatomic distances between the aggregates **12** and the unsubstituted aggregate **11**, and between the unsubstituted and substituted titanoxanes **1** [10] and **2** [10] confirmed that single methylation of the cyclopentadienyl ring had almost no effect on oxo-aggregate structure in the solid state.

4.3. Electronic configuration of the hexanuclear titanoxanes

The essential problem in the description of the electronic structure of the analyzed aggregates is the assignment of the "excess" electrons, that is the electrons in excess of those required for the Ti-cp, Ti–O and Ti–Cl interactions. The number of total available electrons per cluster ranges from 86 for $cp_6Ti_6O_8$ to 94 for $cp_6Ti_6Cl_8$ in a simple valence bond description, where five electrons come from each cp ring, four (the 3d and 4s) from each titanium, four from each oxygen, and five from each chlorine (leaving a lone pair on each oxygen or chlorine atom). Six electrons are required for each Ti–cp bonding, and six electrons also are required for the three Ti–O or Ti–Cl bonds formed by each μ_3-O, or μ_3-Cl atom: therefore 84 electrons are required for each aggregate. The number of "excess" electrons is two for $cp_6Ti_6O_8$, four for $cp_6Ti_6O_2Cl_6$, and ten for $cp_6Ti_6Cl_8$. In molecular orbital calculations, these "excess" electrons are assigned to "excess" orbitals, that is to the orbitals which are in surplus to those required for the Ti–cp, Ti–O or Ti–Cl bondings. These orbitals, which number 12 for the

Table 8
Energy levels of the 12 'excess" orbitals of $Cp_6Ti_6O_{8-n}Cl_n$ clusters ($n = 0, 2, 4, 6, 8$)

$Cp_6Ti_6O_8$ (O_h)		$Cp_6Ti_6O_6Cl_2$ (C_{2h})		$Cp_6Ti_6O_4Cl_4$ (D_{2h})		$Cp_6Ti_6O_2Cl_6$ (C_{2h})		$Cp_6Ti_6Cl_8$ (O_h)	
Orbital	Energy (eV)	Orbital	Energy (eV)	Orbital	Energy (eV)	Orbital	Energy (eV)	Orbital	Energy (eV)
a_{1g}	−11.44	b_g	−10.85	a_g	−10.81	a_g	−10.94	a_{1g}	−11.49
e_g	−9.88	a_g	−10.65	b_{1u}	−10.24	$2a_g$	−10.71	e_g	−10.45
		a_u	−9.91	b_{2g}	−10.10	b_u	−10.20		
t_{2u}	−9.43	b_u	−9.91	$2b_{1u}$	−10.10	b_g	−10.13	t_{2u}	−10.02
		$2a_u$	−9.69	$2a_g$	−10.03	a_u	−10.10		
		$2a_g$	−9.62	b_{3u}	−9.64	$2a_u$	−9.87		
a_{2g}	−8.41	$2b_u$	−9.50	b_{2u}	−9.41	$2b_u$	−9.45	a_{2g}	−9.51
t_{1u}	−8.14	$2b_g$	−8.87	$3a_g$	−9.41	$2b_g$	−8.81	t_{1u}	−8.99
		$3a_u$	−8.34	$2b_{3u}$	−8.64	$3a_g$	−8.71		
		$3a_g$	−8.27	$2b_{2g}$	−8.51	$3a_u$	−8.66		
e_u	−7.29	$3b_g$	−7.92	$3b_{1u}$	−8.07	$4a_g$	−8.49	t_{2g}	−8.17
		$3b_u$	−7.90	$4b_{1u}$	−7.97	$3b_u$	−8.19		
Electronic configuration a_{1g}^2		$b_g^2a_g^2$		$a_g^2b_{1u}^2b_{2g}^12b_{1u}^1$		$a_g^22a_g^2b_u^2b_g^1a_u^1$		$a_{1g}^2e_g^4t_{2u}^4$	

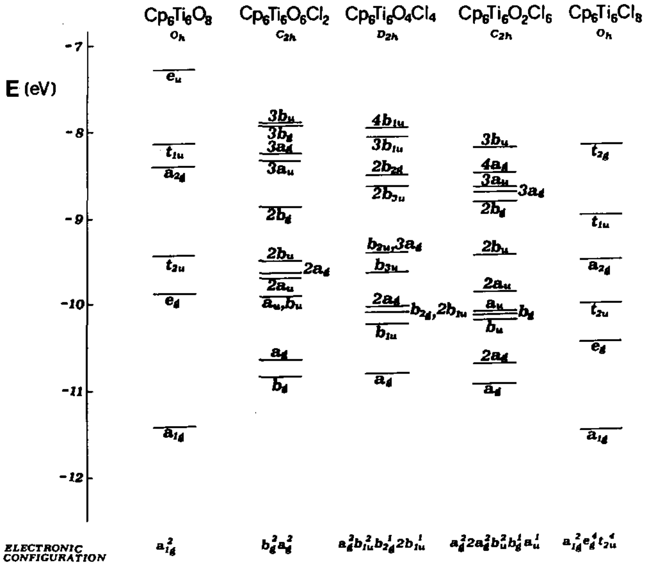

Fig. 5. Energy level diagram for the "excess" orbitals and electronic configuration of $cp_6Ti_6O_{8-n}Cl_n$ ($n = 0, 2, 4, 6, 8$) clusters.

clusters on question, come at an intermediate energy with respect to the bonding and antibonding Ti–cp, Ti–O and Ti–Cl orbitals, and they are mainly titanium d in character.

We start our analysis with $cp_6Ti_6O_8$, whose structure is reported in Fig. 4. The energies of the 12 "excess" orbitals of $cp_6Ti_6O_8$ are shown in Table 8 [1]. Our results are comparable with those obtained by Bottomley and Grein [31]. The main difference is in the highest energy orbital, which we determine to be of symmetry e_u but is e_g, according to Bottomley and Grein. This can probably be ascribed to the different parameters employed in the calculations and does not affect the following discussion. The two "excess" electrons of $cp_6Ti_6O_8$ occupy the a_{1g} orbital, in agreement with the diamagnetism of this cluster. This orbital is essentially metal d in character: it is mainly d_{z^2} arising from the two titanium atoms (Ti_z) lying along the z coordinate and $d_{x^2-y^2}$ from the four titanium atoms (Ti_{xy}) lying in the x–y plane. The lobes pointing into the octahedron are positive, and therefore we can conclude, following Gillespie [32] and Bottomley and Grein [31], that the two "excess" electrons are located in the center of the octahedron. These two electrons therefore are bonding with respect to the Ti–Ti interactions, and this is confirmed by the Mulliken overlap populations, which are 0.02 electrons for each Ti–Ti bond.

The energy level diagram of $cp_6Ti_6Cl_8$ is entirely comparable with that of $cp_6Ti_6O_8$, as expected (Fig. 5). The main difference is in the highest "excess" orbital, which is of t_{2g} symmetry for $cp_6Ti_6Cl_8$. This orbital is lower in energy than e_u since the Cl → Ti interaction is stronger than the O → Ti interaction. $Cp_6Ti_6Cl_8$ has ten "excess" electrons, which should give rise to the electronic configuration $a_{1g}{}^2e_g{}^4t_{2u}{}^4$. However, a Jahn–Teller distortion [33] should occur and the cluster could be diamagnetic. The occupied "excess" orbitals are essentially metal d in character: they are mainly d_{z^2} and/or $d_{x^2-y^2}$ from the six titanium atoms. The analysis of $cp_6Ti_6O_8$ and $cp_6Ti_6Cl_8$ is in agreement with the view advanced by Bottomley and Grein [31] that a general energy level diagram may apply to all the $cp_6M_6A_8$ clusters, at least when the symmetry is octahedral. However, when the symmetry is lowered, we need a different energy level scheme since we cannot explain the diamagnetism of $cp_6Ti_6O_6Cl_2$ and the paramagnetism of $cp_6Ti_6O_4Cl_4$ with the energy level order found for the octahedral aggregates. The energy level schemes calculated for $cp_6Ti_6O_6Cl_2$ and $cp_6Ti_6O_4Cl_4$ are listed in Table 8. The aggregate $cp_6Ti_6O_6Cl_2$ shows C_{2h} symmetry and has four "excess" electrons. The ground state therefore is $b_g{}^2a_g{}^2$, in agreement with the diamagnetism of this compound. The a_g orbital is mainly d_{z^2} from the two Ti_z atoms and $d_{x^2-y^2}$ from the four Ti_{xy} atoms and it is bonding with respect to each Ti–Ti interaction. The b_g orbital is mainly d_{z^2} from the two Ti_z atoms and a combination of $d_{x^2-y^2}$ and d_{z^2} from the four Ti_{xy} atoms. It is slightly bonding with respect to each Ti_{xy}–Ti_z interaction but is antibonding with respect to the Ti_{xy}–Ti_{xy} interactions. Consequently, the Ti_{xy}–Ti_z overlap populations assume positive values (0.04 and 0.08 electron, the difference being due to the asymmetry induced by the presence of the chlorine atoms), while the Ti_{xy}–Ti_{xy} overlap populations are slightly negative. The geometry of this cluster requires a Ti_{xy}–Ti_z distance shorter than the Ti_{xy}–Ti_{xy} distance, in agreement with the calculated overlap populations.

The aggregate $cp_6Ti_6O_4Cl_4$ shows D_{2h} symmetry and has six "excess" electrons. From Table 8, we can see that the b_{2g} and $2b_{1u}$ orbitals are at the same energy, although the D_{2h} symmetry group does not show degenerate representations; therefore these orbitals exhibit an accidental degeneration. The b_{2g} orbital is the sum of $d_{x^2-y^2}$ from the two Ti_z atoms, while the $2b_{1u}$ is the difference of the same orbitals. The two Ti_z atoms do not interact at all, since the distance between them is very long (5.61 Å). This could be the reason for the degeneration of the b_{2g} and $2b_{1u}$ orbitals. The ground state of $cp_6Ti_6O_4Cl_4$ therefore is $a_g{}^2b_{1u}{}^2b_{2g}{}^12b_{1u}{}^1$, and this compound should be paramagnetic per two unpaired electrons, in agreement with the experimental data ($\mu = 2.89\ \mu_B$ at 290 K). The a_g and b_{1u} orbitals are mainly $d_{x^2-y^2}$ and d_{z^2} from the four Ti_{xy} atoms. a_g is bonding with respect to each Ti_{xy}–Ti_{xy} interaction while b_{1u} is bonding with respect

---

[1] Tables of extended Hückel parameters are available from the authors.

to two Ti_{xy}–Ti_{xy} interactions and antibonding with respect to the other two Ti_{xy}–Ti_{xy} interactions. We note that there are no Ti_{xy}–Ti_z interactions in the occupied orbitals, in agreement with the experimental evidence that the Ti_{xy}–Ti_z distance is longer than the Ti_{xy}–Ti_{xy} distance. The Ti–Ti overlap populations are slightly negative, except for the two Ti_{xy}–Ti_{xy} populations of 0.13 electron relative to the Ti_{xy}–Ti_{xy} bonding interactions.

To complete our analysis, we have performed calculations also on $cp_6Ti_6O_2Cl_6$, whose geometry has been deduced from those of the other clusters of the series. This compound has C_{2h} symmetry and the energy level scheme is shown in Table 8. The eight "excess" electrons should give rise to the electronic configuration $a_g{}^2 2a_g{}^2 b_u{}^2 b_g{}^1 a_u{}^1$. The energies of the b_g and a_u orbitals, even though they are not equal, are very close, and therefore the cluster should be paramagnetic with two unpaired electrons. However, the possibility of a more complex magnetic behavior of $cp_6Ti_6O_2Cl_6$ cannot be discarded, since the energy gap between the b_g and a_u orbitals rises slightly if we assume a different geometry.

In Table 9 we list the net atomic charges for the analyzed clusters. Small differences in the oxygen or chlorine charges have been averaged. In the octahedral compounds, all six titanium atoms show the same charge, while in the aggregates with a distorted octahedral structure we have a different charge on the Ti_z atoms from that on the Ti_{xy} atoms. Finally, we note that, as expected, there is a progressive reduction in the charge on the titanium atoms, due to the substitution of oxygen with chlorine atoms, on going from $cp_6Ti_6O_8$ to $cp_6Ti_6Cl_8$. The charges on the other atoms are in keeping with their electronegativity.

The electronic structures of the $[cp_6Ti_6X_8]$ compounds provide fundamental information on their properties and ultimately on their chemical behavior. The 12 excess orbitals mainly derived from the d metal orbitals may behave as a metallic band with potential for electronic storage and corresponding electron release processes. The population and depopulation of such "excess orbitals" should not significantly affect the skeleton, the molecule maintaining intact its framework while undergoing electron exchange processes. (Indirect evidence for this is provided by the presence of the same skeleton for a different number of electrons for the aggregate). Owing to these features, a compound of the type $cp_6Ti_6X_8$ may find use as molecular batteries. The possible functionalization at the triangle faces of such octahedral structures, and solubility of the compounds in hydrocarbons makes these molecules particularly attractive for reactivity studies.

Acknowledgments

We thank the Fonds National Suisse de la Recherche Scientifique, the Progetto Finalizzato Consiglio Nazionale delle Ricerche, and COST (European Program for Scientific Research) for financial support.

References and notes

[1] V. Day and W.G. Klemperer, *Science, 228* (1985) 533.

[2] (a) M.T. Pope, *Heteropoly and Isopoly Oxometallates*, Springer, Berlin, 1983; (b) H.T. Evans, *Perspect. Struct. Chem., 4* (1971) 1; (c) P. Souchay, *Pure Appl. Chem., 6* (1963) 61; (d) V. Day, W.G. Klemperer and D.J. Maltbie, *J. Am. Chem. Soc., 109* (1987) 2991; (e) V. Day, W.G. Klemperer and D.M. Millar, *J. Am. Chem. Soc., 107* (1985) 8262; (f) V. Day, W.G. Klemperer and D.J. Maltbie, *Organometallics, 4* (1985) 104; (g) C.W. Earley, W.G. Klemperer and D.J. Maltbie, *J. Am. Chem. Soc., 107* (1985) 8261.

[3] (a) C.L. Hill, in *Activation and Functionalization of Alkanes*, Wiley, New York, 1989, Chapter 8; (b) C.L. Hill, *J. Am. Chem. Soc., 108* (1986) 3528.

[4] (a) T.M. Che, V.W. Day, L.C. Francescon, M.F. Fredrich, W.G. Klemperer and W. Shum, *Inorg. Chem., 24* (1985) 4055, and references cited therein; (b) V.W. Day, T.A. Eberspacher, W.G. Klemperer and C.W. Park, *J. Am. Chem. Soc., 115* (1993) 8469, and references cited therein.

[5] (a) Y. Iwasaure, Adv. Catal., 35 (1987) 187; (b) C. Terrier-Youngs, F. Correa, D. Pioch, R.L. Burwell and D.F. Shriver, *Organometallics, 2* (1983) 898.

[6] (a) D.R. Illrich, *J. Non-Cryst. Solids, 100* (1988) 174; (b) V. Day, W.G. Klemperer and D.M. Millar, *Materials Research Society Symp. Proc.*, Vol. 73, Materials Research Society, Pittsburgh, PA, 1986, p. 15; (c) W.G. Klemperer and S.D. Ramamurth, *Better Ceramics through Chemistry Materials Research Society Symp. Proc.*, Vol. 121, Materials Research Society, Pittsburgh,

Table 9
Net atomic charges (electronic units) of $Cp_6Ti_6O_{8-n}Cl_n$ clusters ($n = 0, 2, 4, 6, 8$)

	Net atomic charge of the following				
	$Cp_6Ti_6O_8$	$Cp_6Ti_6O_6Cl_2$	$Cp_6Ti_6O_4Cl_4$	$Cp_6Ti_6O_2Cl_6$	$Cp_6Ti_6Cl_8$
Ti_z	+2.28	+1.85	+1.78	+1.51	+1.02
Ti_{xy}	+2.28	+2.11	+1.66	+1.27	+1.02
O	−1.24	−1.27	−1.22	−1.30	
Cl		−0.41	−0.37	−0.38	−0.39
Cp_z	−0.63	−0.54	−0.76	−0.66	−0.50
Cp_{xy}	−0.63	−0.66	−0.58	−0.48	−0.50

PA, 1988, p. 1; (d) H. Reuter, *Adv. Mater., 3* (1991) 258; (e) M. Guglielmi and G. Cartiran, *J. Non-Cryst. Solids, 100* (1988) 16; (f) C.J. Blinker, *J. Non-Cryst. Solids, 101* (1988) 31; (g) J. Livage, Materials Research Society Symp. Proc., Vol. 73, Materials Research Society, Pittsburgh, PA, 1986, 717, and references cited therein.

[7] F. Bottomley and L. Sutin, *Adv. Organomet. Chem., 28* (1988) 339, and references cited therein.

[8] A. Roth, C. Floriani, A. Chiesi-Villa and C. Guastini, *J. Am. Chem. Soc., 108* (1986) 6823.

[9] (a) A.C. Skapski, P.G.H. Troughton and H.H. Sutherland, *J. Chem. Soc., Chem. Commun.*, (1968) 1418; (b) A.C. Skapski and P.G.H. Troughton, *Acta Crystallogr., Sect. B26* (1970) 716; (c) J.L. Petersen, *Inorg. Chem., 19* (1980) 181.

[10] (a) P. Corradini and G. Allegra, *J. Am. Chem. Soc., 81* (1959) 5510; (b) U. Thewalt and D. Schomburg, *J. Organomet. Chem., 127* (1977) 169; (c) R.D. Gorsich, *J. Am. Chem. Soc., 82* (1960) 4211.

[11] T. Carofiglio, C. Floriani, A. Sgamellotti, M. Rosi, A. Chiesi-Villa and C. Rizzoli, *J. Chem. Soc., Dalton Trans.*, (1992) 1081.

[12] (a) R.S.P. Coutts, R.L. Martin and P.C. Wailes, *Aust. J. Chem., 24* (1971) 2533; (b) S. Gambarotta, C. Floriani, A. Chiesi-Villa and C. Guastini, *J. Am. Chem. Soc., 105* (1983) 7295.

[13] S.L. Lawton and R.A. Jacobson, TRACER, a Cell Reduction Program Ames laboratory, Iowa State University of Science and Technology, Ames, IA, 1965.

[14] M.S. Lehmann and F.K. Larsen, *Acta Crystallogr., Sect. A30* (1974) 580.

[15] Data reduction, structure solution, and refinement were carried out on a GOULD 32/77 computer using the following: G. Sheldrick, SHELX-76 *System of Crystallographic Computer Programs*, University of Cambridge, Cambridge, Cambs., 1976.

[16] A.J.C. Wilson, *Nature, 150* (1942) 151.

[17] F. Uguzzoli, *Comput. Chem., 11* (1987) 109.

[18] *International Tables for X-ray Crystallography*, Vol. IV, Kynoch Press, Birmingham, 1974, (a) p. 99; (b) p. 149.

[19] R.F. Stewart, E.R. Davidson and W.T. Simpson, *J. Chem. Phys., 42* (1965) 3175.

[20] (a) R. Hoffmann, *J. Chim. Phys., 39* (1963) 1397; (b) R. Hoffmann and W.N. Lipscomb, *J. Chim. Phys., 36* (1962) 2179; (c) R. Summerville and R. Hoffmann, *J. Am. Chem. Soc., 98* (1976) 7240.

[21] K. Tatsumi, A. Nakamura, P. Hoffmann, P. Stauffert and R. Hoffmann, *J. Am. Chem. Soc., 107* (1985) 4440.

[22] J.C. Huffmann, J.G. Stone, W.C. Krusell and K.G. Caulton, *J. Am. Chem. Soc., 99* (1977) 5829.

[23] (a) F. Bottomley, E.C. Ferris and P.S. White, *Organometallics, 9* (1990) 1166; (b) F. Bottomley, P.D. Boyle, S. Karslioglu and R.C. Thompson, *Organometallics, 12* (1993) 4090, and references cited therein; (c) F. Bottomley and R.W. Day, *Can. J. Chem., 70* (1992) 1250, and references cited therein; (d) F. Bottomley, *Polyhedron, 11* (1992) 1707, and references cited therein.

[24] W.A. Herrmann, R.W. Albach and J. Behm, *J. Chem. Soc., Chem. Commun.*, (1991) 367.

[25] M. Kilner, G. Parkin and A.G. Talbot, *J. Chem. Soc., Chem. Commun.*, (1985) 34.

[26] (a) T. Fjelberg, A. Haaland, B.E.R. Schilling, M.F. Lappert and A.J. Thorne, *J. Chem. Soc., Dalton Trans.*, (1986) 1551; (b) E.J. Roskamp and F. Pedersen, *J. Am. Chem. Soc., 109* (1987) 3152, 6551.

[27] J.C. Hoffmann, J.G. Stone, W.C. Krussel and K.G. Caulton, *J. Am. Chem. Soc., 99* (1977) 5829.

[28] F. Bottomley, D.F. Drummond, G.O. Egharevba and P.S. White, *Organometallics, 5* (1986) 1620.

[29] R.C. Fay, *Coord. Chem. Rev., 45* (1982) 9.

[30] F. Bottomley, D.E. Paesz and P.S. White, *J. Am. Chem. Soc., 104* (1982) 5651.

[31] F. Bottomley and F. Grein, *Inorg. Chem., 21* (1982) 4170.

[32] R.J. Gillespie, *Chem. Soc. Rev., 8* (1979) 315.

[33] R.W. Jotham and S.F.A. Kettle, *Inorg. Chim. Acta, 5* (1971) 183.